nature neuroscience

ARTICLES

Developmental switch from GABA to glycine release in single central synaptic terminals

Junichi Nabekura[1,2,5] Shutaro Katsurabayashi[1,5], Yasuhiro Kakazu[1], Shumei Shibata[1], Atsushi Matsubara[3], Shozo Jinno[4], Yoshito Mizoguchi[1], Akira Sasaki[3] & Hitoshi Ishibashi[1]

Early in postnatal development, inhibitory inputs to rat lateral superior olive (LSO) neurons change from releasing predominantly GABA to releasing predominantly glycine into the synapse. Here we show that spontaneous miniature inhibitory postsynaptic currents (mIPSCs) also change from GABAergic to glycinergic over the first two postnatal weeks. Many 'mixed' mIPSCs, resulting from co-release of glycine and GABA from the same vesicles, are seen during this transition. Immunohistochemistry showed that a large number of terminals contained both GABA and glycine at postnatal day 8 (P8). By P14, both the content of GABA in these mixed terminals and the contribution of GABA to the mixed mIPSCs had decreased. The content of glycine in terminals increased over the same period. Our results indicate that switching from GABAergic to glycinergic inputs to the LSO may occur at the level of a single presynaptic terminal. This demonstrates a new form of developmental plasticity at the level of a single central synapse.

GABA and glycine are the major inhibitory transmitters in the mammalian central nervous system. Although they act at separate receptors, they can be co-released from single synaptic terminals projecting onto spinal motor neurons and brainstem trigeminal neurons[1,2]. Postsynaptic clusters of both glycine and $GABA_A$ receptors appear to be co-localized at the subsynaptic membrane[3,4]. Furthermore, mIPSCs recorded from spinal neurons include both GABAergic and glycinergic components, suggesting that both GABA and glycine are co-released from a single synaptic vesicle[5,6]. Hence, at spinal cord synapses, GABA and glycinergic transmission is closely related, and this could have important implications for the strength and timing of motor neuron inhibition[7].

The coordinated combination of GABAergic and glycinergic inhibitory transmission is also functionally critical in the lateral and medial superior olive auditory relay neurons (LSO and MSO neurons, respectively)[8,9]. In the normal development of the auditory system, inhibitory synaptic transmission in the LSO and MSO changes from being predominantly GABAergic to being predominantly glycinergic[8,9]. Structural reorganization of the inhibitory synapses between the medial nucleus of the trapezoidal body (MNTB) and the LSO also occur throughout development[10], and it is unclear whether this switch from GABA to glycine occurs via a selective loss of GABAergic synapses and an increase in glycinergic synapses, or whether this transmitter switch occurs at individual synapses. Developmental changes in receptor subunit expression patterns have been observed in the LSO[11], but there have been no reports of a presynaptic change in the nature of the released neurotransmitter at the level of a single synapse. In the present study, we further elucidate the mechanisms contributing to this neurotransmitter switch, particularly focusing on whether presynaptic changes occur and whether they occur at single synapses.

RESULTS

Evoked IPSCs (eIPSCs) were recorded from LSO neurons in response to electrical stimulation of the ventromedial part of the LSO slice preparation. Both CNQX (10^{-5} M) and APV (10^{-5} M) were added to the external solution to block glutamatergic responses. In LSO neurons from P2 rats, bicuculline (10^{-5} M) inhibited the eIPSC by about 70%, but only caused a mild (about 15%) inhibition in P14 rats (**Fig. 1a**,**b**). The bicuculline-insensitive component of the eIPSC was completely abolished, at all ages, by adding strychnine (10^{-6} M). The inhibitory effects of bicuculline on muscimol and glycine responses were stable in potency throughout development (**Fig. 1c**). Thus, inhibitory synaptic transmission to LSO neurons changed from predominantly GABAergic to predominantly glycinergic during development. The switch is evident by P7, which is somewhat earlier than observed in the gerbil LSO[8], although it is virtually completed by this time for inhibitory inputs to the rat MSO[9].

To elucidate the underlying cause of this switch from predominantly GABAergic to predominantly glycinergic inputs, we concentrated on the nature of miniature IPSCs (mIPSCs), which are considered to be single quantal events[12,13]. We mechanically dissociated LSO neurons with adherent presynaptic terminals[14] (**Fig. 2a**) and recorded mIPSCs at a V_H of –60 mV in the presence of CNQX (10^{-5} M), APV (10^{-5} M) and tetrodotoxin (TTX; 3×10^{-7} M). This preparation allows us to measure spontaneous synaptic currents under good space-clamp conditions and without complications from other neurons or glia[14]. We

[1]Department of Cellular and System Physiology, Graduate School of Medical Sciences, Kyushu University, Fukuoka 812-8582, Japan. [2]Department of Developmental Physiology, National Institute for Physiological Sciences, Okazaki 444-8585, Japan. [3]Department of Otorhinolaryngology, School of Medicine, Hirosaki University, Hirosaki 036-8562, Japan. [4]Department of Anatomy and Neurobiology, Graduate School of Medical Sciences, Kyushu University, Fukuoka 812-8582, Japan. [5]These authors contributed equally to this work. Correspondence should be addressed to J.N. (nabekura@nips.ac.jp).

Published online 21 December 2003; doi:10.1038/nn1170

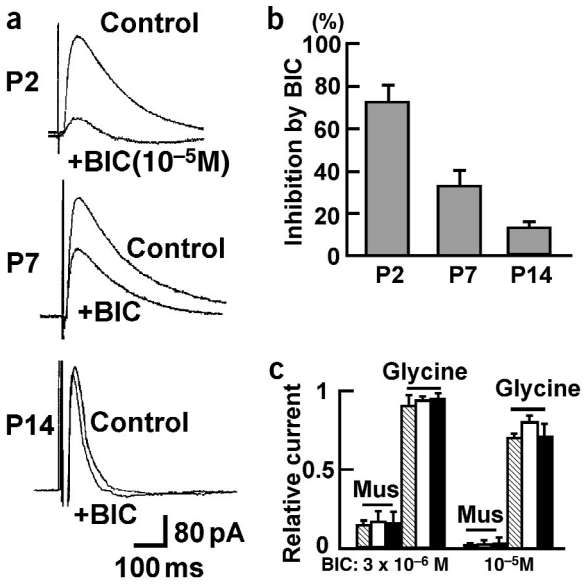

Figure 1 Developmental change in the bicuculline sensitivity of IPSCs recorded in LSO neurons in response to electrical stimulation of the ventromedial aspect of the LSO brain slice. (**a**) Five representative averaged evoked IPSCs, recorded from P2, P7 and P14 rats, in the absence (Control) and presence of 10^{-5} M bicuculline (+BIC). We used bicuculline rather than strychnine to discriminate between $GABA_A$ and glycine receptor responses because the potency of strychnine on muscimol (which affect $GABA_A$ receptors) responses varied during development (unpublished data). (**b**) Mean data showing the relative inhibition of eIPSCs by bicuculline, in LSO neurons from different developmental stages ($n = 6$, respectively). Evoked IPSCs were recorded using standard whole-cell patch-clamp techniques. V_H was 0 mV. (**c**) Inhibition of 10^{-5} M muscimol and 3×10^{-5} M glycine evoked responses by 3×10^{-6} and 10^{-5} M bicuculline, in LSO neurons from P0–2 (strip columns), P6–8 (open columns) and P14–16 (closed columns) rats. Response amplitudes are plotted relative to that observed in the absence of bicuculline ($n = 5$ or 6 in each case). The relative inhibitory effect of bicuculline on $GABA_A$ and glycine receptor mediated responses was constant throughout development.

initially pharmacologically isolated GABAergic and glycinergic components of mIPSCs in LSO neurons from P6–7 rats (**Fig. 2b**, left). In the presence of bicuculline (5×10^{-6} M), glycinergic mIPSCs were observed with a relatively fast decay time constant (fit from 90–10% of the mIPSC amplitude, $\tau_{gly} = 7.2 \pm 1.3$ ms, mean ± s.e.m., $n = 5$ neurons, **Fig. 2c,d**). In the same neurons, GABAergic mIPSCs, in the presence of strychnine (3×10^{-7} M), were observed with a much slower decay time constant ($\tau_{GABA} = 73.6 \pm 4.5$ ms, $n = 5$, **Fig. 2c,d**). In three other neurons, the mIPSC decay in the presence of another selective $GABA_A$ antagonist, SR-95531, was fit with a similar time constant as observed in the presence of bicuculline ($\tau_{gly} = 8.3 \pm 2.2$ ms). These results are consistent with previous reports that GABAergic mIPSCs are characterized by a longer current decay time than are glycinergic mIPSCs[6,15,16] and indicate that the mIPSCs contain both $GABA_A$ receptor– and glycine receptor–mediated components. Indeed, in control conditions, mIPSCs with two components were also detected (**Fig. 2b**, right). The decay of these dual-component, 'mixed' mIPSCs was fit with the sum of two exponentials, a τ_{fast} and τ_{slow}, which were 6.2 ± 0.9 ms and 58.7 ± 10.3 ms, respectively ($n = 5$; **Fig. 2d**). These time constants were very similar to the pharmacologically isolated τ_{gly} and τ_{GABA}, and this excellent agreement between τ_{slow} and τ_{GABA}, and between τ_{fast} and τ_{gly} was found throughout development. In neurons from P1–2 rats, τ_{fast} was 7.3 ± 3.4 ms ($n = 5$) and τ_{gly} was 8.3 ± 2.5 ms ($n = 5$), whereas τ_{slow} was 84.2 ± 8.5 ms ($n = 5$) and τ_{GABA} was 92.9 ± 10.2 ms ($n = 5$). In neurons from older rats (P16–17), τ_{fast} was 3.4 ± 1.4 ms ($n = 5$) and τ_{gly} was 3.7 ± 1.5 ms ($n = 5$), whereas τ_{slow} was 42.2 ± 6.4 ms ($n = 5$) and τ_{GABA} was 38.2 ± 7.2 ms ($n = 5$). These results show that these mixed mIPSCs reflect co-release of GABA and glycine from a single vesicle. They also show how the mIPSC decay constants get faster during development, presumably reflecting changes in receptor subunit composition[17].

Just as was observed for the eIPSCs, the chemical nature of mIPSCs also changed from predominantly GABAergic to predominantly glycinergic (**Fig. 3**). In the absence of any strychnine or

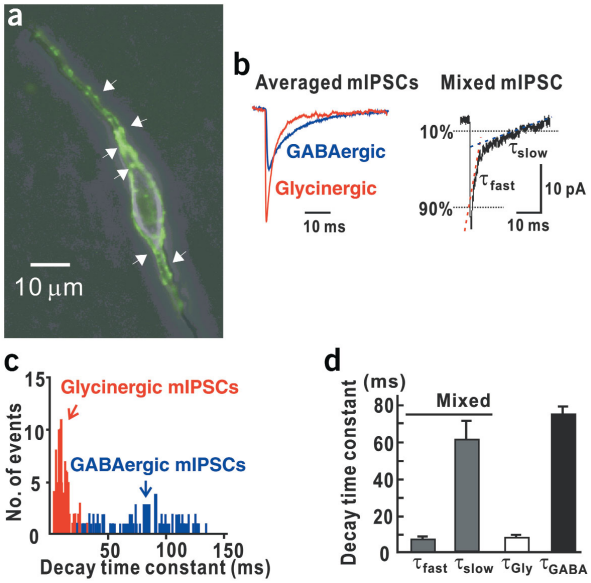

Figure 2 Pharmacological and kinetic isolation of GABAergic, glycinergic and mixed mIPSCs in voltage-clamped, isolated LSO neurons. (**a**) Photograph of a mechanically dissociated LSO neuron from P7 rats showing adherent functional synaptic boutons stained green with FM1-43. FM1-43 (1 mM) was added to the perfusate with 20 mM K^+ for 3 min, then washed out with Ca^{2+}-free, standard extracellular solution. Arrowheads indicate examples of stained synaptic boutons. (**b**) Left, averaged mIPSCs recorded in the presence of strychnine (300 nM, GABAergic mIPSC, blue, $n = 121$) and in the presence of bicuculline (5 µM, glycinergic mIPSC, red, $n = 96$) from a LSO neuron isolated from a P7 rat. Right, a 'mixed' mIPSC with a decay composed of both fast and slow components, recorded in the absence of any receptor antagonists in a LSO neuron from a P7 rat. (**c**) Distribution of the decay time constants of GABAergic (blue bars, strychnine 300 nM) and glycinergic mIPSCs (red bars, bicuculline, 5 µM) in an LSO neuron from P7 rat. Bin size, 1 ms. (**d**) Mean decay time constants for the three types of mIPSCs (mean ± s.e.m., $n = 5$ in each case). The mixed mIPSCs were fit by the sum of two exponential equations with time constants τ_{fast} and τ_{slow}, that corresponded to the decay time constants of the pharmacologically isolated glycinergic (τ_{gly}) and GABAergic (τ_{GABA}) mIPSCs, respectively.

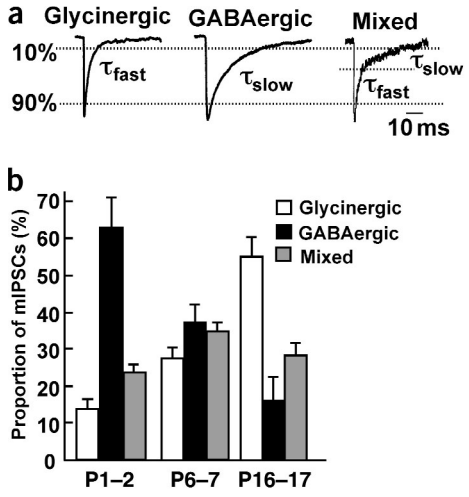

Figure 3 Developmental change in mIPSCs recorded in isolated LSO neurons. (**a**) Typical examples of GABAergic, glycinergic and mixed mIPSCs in a P6 LSO neuron. Horizontal bars indicate how the mIPSC decay, from 90% to 10% of the peak amplitude, was fit with one or two exponential functions (see **Fig. 2b**). The traces were obtained from a P6 LSO neuron. (**b**) Relative proportion of GABAergic (closed columns), glycinergic (open columns) and mixed mIPSCs (gray columns) in LSO neurons from P1–2, P6–7 and P16–17 rats. The proportion of mIPSCs of each type are expressed relative to the total number of mIPSCs recorded in each neuron (>200 events in each neuron), and are the mean ± s.e.m. of results from 10–12 neurons in each age group.

bicuculline, individual mIPSCs which were fit to either τ_{fast} or τ_{slow} were defined as glycinergic and GABAergic events, respectively (**Fig. 3a**). In P1–2 neurons, the proportion of total mIPSCs whose decay times indicated that they were GABAergic was 63.0 ± 7.5%, and in neurons from P16–17 the proportion was 16.0 ± 6.5%. At the same ages the proportions of glycinergic mIPSCs were 13.6 ± 2.8% and 55.3 ± 5.2%, respectively (**Fig. 3b**). The remainder of the mIPSCs had dual-component decay times (mixed mIPSCs). The incidence of these mixed mIPSCs was highest at P6–7 where they comprised 34.9 ± 2.5% of all mIPSCs ($n = 10$). In P1–2 and P16–17 rats, mixed mIPSCs comprised 23.4 ± 2.3% ($n = 10$) and 28.6 ± 3.2% ($n = 12$), respectively, of the total mIPSCs.

The mixed mIPSCs result from co-release of GABA and glycine from a single vesicle. To address whether the response to single vesicles shows a developmental change from GABAergic to glycinergic, we analyzed the relative contribution of the GABAergic (y_{GABA}) and glycinergic (y_{gly}) components to the total peak amplitude (y) of the mixed mIPSCs (**Fig. 4a**). If neurotransmitter switching also occurs at the level of single synapses, the GABAergic component in the mixed mIPSCs would be expected to decrease with age and the glycinergic component would increase. The absolute amplitude of the glycinergic component increased with age: 15.6 ± 3.2 pA at P1–2, 27.9 ± 3.6 pA at P6–7 and 43.4 ± 8.2 pA at P16–17 (n = 10–12 neurons at each age). The amplitude of the GABAergic component also increased from P1–2 (10.5 ± 2.9 pA, $n = 10$) to P6–7 (19.0 ± 1.5 pA, $n = 10$), before declining again in older rats (13.3 ± 1.7 pA at P16–17, $n = 12$, **Fig. 4c**). The relative contribution of the GABAergic component to the total mixed mIPSC amplitude (y_{GABA}/y) was not significantly different between P1–2 and P6–7 rats, but was decreased in older (P16–17) rats (38.9 ± 3.5% at P1–2, 53.2 ± 5.9% at P6–7 and 25.8 ± 3.9% at P16–17, **Fig. 4b,d**). Thus, the contribution of GABA to the response to a single vesicle declines in older rats, whereas that of glycine increases, consistent with neurotransmitter switching occurring at a single synapse.

The above results demonstrate a developmental switch from GABAergic to glycinergic neurotransmission at single synapses but do not distinguish whether this change occurs presynaptically (that is, a single terminal switches from GABA to glycine release), or postsynaptically (that is, a change in subsynaptic receptors from $GABA_A$ to glycine[8,11] with a constant co-release of GABA and glycine throughout development[16]), or a combination of both. The mean responses of LSO neurons to exogenous GABA and glycine were not significantly different throughout development. Specifically, GABA (3×10^{-5} M) induced an inward current at a V_H of –60 mV of 305 ± 68 pA in neurons from P0–2 rats, 409 ± 38 pA from P7 rats and 364 ± 82 pA from P14 rats ($n = 5$ or 6 neurons at each age). At the same ages the response to glycine (10^{-4} M) was 297 ± 57 pA at P0–2, 349 ± 84 pA at P7 and 305 ± 58 pA at P14 ($n = 5$ or 6). Therefore, there does not seem to be any gross developmental change in the response of the extrasynaptic receptors, although this may not reflect what is occurring at the subsynaptic receptors.

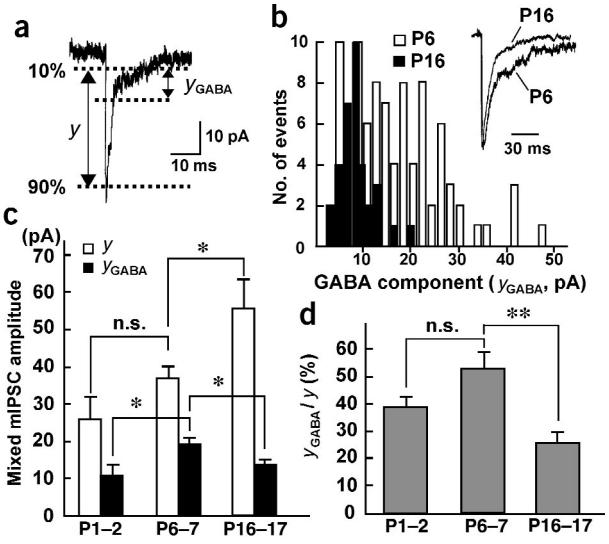

Figure 4 Developmental decrease in the contribution of the GABAergic component to mixed mIPCSs. (**a**) Example of a mixed mIPSC to illustrate the meaning of y (the peak mIPSC amplitude) and y_{GABA} (the amplitude of the mIPSC due to the GABAergic component). Individual events were fit with the double exponential function: $y = y_0 + y_{fast}\, e^{(-x/\tau fast)} + y_{slow}\, e^{(-x/\tau slow)}$, in which y_{fast} and y_{slow} were defined as $y_{glycine}$ and y_{GABA} and their sum as y. (**b**) Distribution of y_{GABA} in mixed mIPSCs from typical P6 (open bars) and P16 (black bars) LSO neurons. mIPSCs from P6 and P16 neurons were scaled so as to make their peak amplitudes equivalent. Note that the GABAergic component (y_{GABA}) of the mixed mIPSCs in P16 LSO neurons was smaller than that in P6 LSO neurons. Bin size, 2 pA. (**c**) Comparison of the mean absolute peak amplitude of mixed mIPSCs (y, open bars) and the mean amplitude of the GABAergic component (y_{GABA}, closed bars) in different age groups. Note the steady increase in y throughout development and the smaller contribution of y_{GABA} in the P16–17 rats. (**d**) Relative contribution of the GABAergic component to the peak amplitude of the mixed mIPSCs (y_{GABA}/y) at different developmental stages. Note the marked decrease in y_{GABA}/y after P6–7.

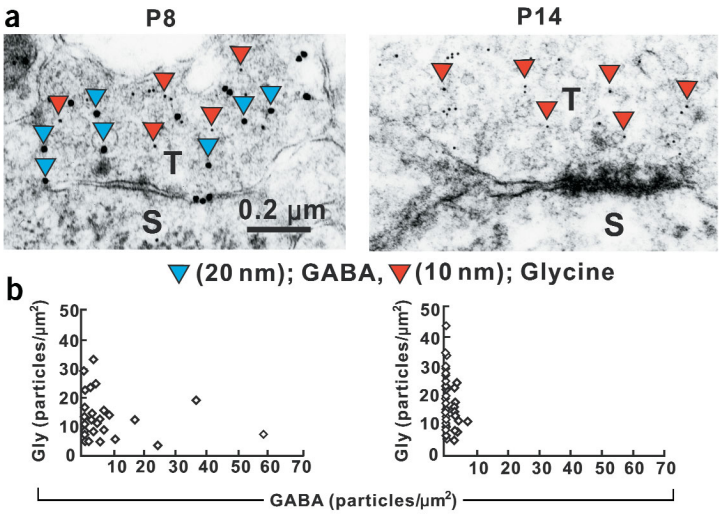

Figure 5 Quantitative analysis of GABA and glycine content in presynaptic terminals using immunogold staining and electron microscopy. (**a**) Typical electron micrographs of a synapse on to an LSO neuron; in a P8 (left) and P14 (right) rat. The large (20 nm) gold particles indicated with blue arrow heads are coated with antibodies specific to GABA, whereas the smaller (10 nm) gold particles are coated with antibodies to glycine (red arrowheads). T, presynaptic terminal; S, soma of postsynaptic cell. (**b**) Summary of group data from the immunogold experiments in P8 (left) and P14 (right) LSO neurons. Number of GABA-reactive particles/μm^2 in each inhibitory synapse is plotted against the number of glycine-reactive gold particles observed in the same synapse (total number of terminal micrographs observed were 58 from three P8 rats, and 80 from three P14 rats). Note that all inhibitory synapses observed contained glycine, but significant quantities of GABA were only colocalized in these synapses from the P8 neurons. The number of glycine particles was greater in P14 synapses than in P8 synapses ($P < 0.05$, unpaired *t*-test). The specificity of each antibody was examined using control experiments (**Supplementary Fig. 2**).

We also examined any presynaptic changes during development by looking directly at the composition of transmitters in single presynaptic terminals using an immunogold technique and electron microscopy (**Fig. 5**). Many terminals showed a background stain of about 1–5 gold particles/μm^2, so only terminals with a total number of GABA- and glycine-reactive particles greater than this background level were considered to be clearly inhibitory synapses and included in the subsequent analysis (**Supplementary Fig. 1** online). At P8, 38/58 terminals satisfied this criterion, and at P14, 41/80 terminals were included. At P14, the density of glycine-reactive gold particles in a single terminal was 18.6 ± 1.5/μm^2 (mean ± s.e.m., $n = 41$), which was significantly larger than observed at P8 (11.8 ± 1.2 particles/μm^2, $n = 38$, $P < 0.05$, unpaired *t*-test, **Fig. 5b**). In contrast, the GABA particle density in single terminals significantly decreased over the same period, from 4.9 ± 1.8/μm^2 at P8 ($n = 38$) to 0.9 ± 0.30/μm^2 at P14 ($n = 41$; $P < 0.05$). The percentage of terminals where both GABA- and glycine-reactive gold particles were observed, decreased from 50% at P8 (19/38 terminals) to 32% (13/41) at P14. Hence, switching of inhibition from GABAergic to glycinergic is also reflected in an increase in glycine content in terminals, a decrease in the proportion of terminals containing GABA, and a decrease in the extent of GABA in terminals where both transmitters are present.

One mechanism that potentially could decrease the amount of GABA in single presynaptic terminals is a decrease in the synthesis of GABA in the LSO. To investigate this possibility, we used immunohisto-chemistry and confocal microscopy to examine levels of the GABA synthesizing enzyme, glutamic acid decarboxylase (GAD). For comparison, we also stained for glycine in these experiments. The glycine antibody staining in the LSO markedly increaseed in intensity during development, whereas GAD antibody staining (which recognizes both GAD 65 and GAD 67) seemed to decrease in intensity over the same period (**Fig. 6**). At higher resolution (**Fig. 6g–l**), similar changes in the number of GAD- and glycine-reactive puncta are seen, although several terminals still showed clear GAD staining even at P18 (**Fig. 6k**). This developmental pattern of glycine staining parallels that observed in the immunogold experiments (**Fig. 5**). The decrease in GAD staining suggests that a decrease in GABA synthesis contributes to the decrease in the GABA content in individual terminals.

Finally, we examined whether the extent of occupation of the postsynaptic GABA receptor clusters changes during the transitional period when the contribution of GABA to mIPSCs is changing. In three out of seven neurons from P6 rats, diazepam (3×10^{-7} M) increased the mean amplitude of mIPSCs by about 6–16%. This suggests that, for these three neurons, the GABA content in a single vesicle does not saturate the subsynaptic $GABA_A$ receptors. Given that the concentration of GABA in the synaptic cleft at individual release sites is typically sufficient to saturate postsynaptic $GABA_A$ receptor clusters in central neurons[18], this result further supports the decreased content of GABA in single vesicles and suggests that the presynaptic decreases in GABA may occur before significant decreases in the number of postsynaptic receptors[11].

DISCUSSION

In the present study, we used both electrophysiological analysis of mIPSCs and immunohistochemistry to show that the neurotransmitter phenotype of single presynaptic inhibitory terminals changes from GABAergic to glycinergic during the first two postnatal weeks. An initial period of expansion of both MNTB terminal arborizations and LSO dendrites in the first one or two postnatal weeks is followed by a refinement of these processes and a loss of synaptic specializations[19]. Recent studies indicate that the functional elimination of inhibitory inputs from MNTB to the LSO may occur before the structural changes, even within the first two weeks[20]. If synapse elimination and refinement were solely responsible for this presynaptic switch, terminals would need to be selectively eliminated based on subtle differences in their relative presynaptic GABA and glycine content, and sequentially replaced with glycinergic terminals containing an increasing amount of glycine and a decreasing amount of GABA. We strongly favor a much simpler hypothesis; that the concentration of glycine increases, while that of GABA decreases, in single terminals. This inference is also supported by the decrease in GAD levels (**Fig. 6**). Considering that the vesicular inhibitory amino acid transporter (VIAAT) can pump both GABA and glycine into the presynaptic vesicles[21], this developmental change in terminal GABA/glycine content is then reflected in the vesicular content of GABA/glycine and the

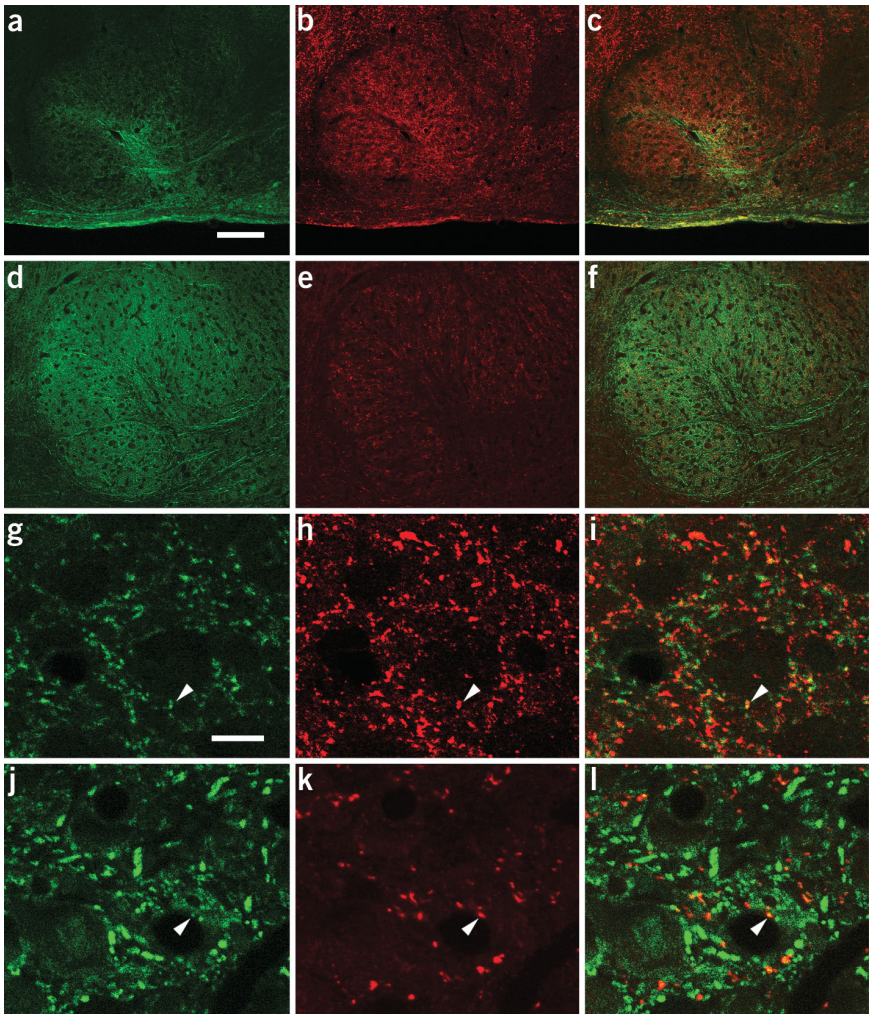

Figure 6 Immunohistochemical staining of GAD and glycine in the developing LSO. Immunofluorescent double-labeled confocal laser scanning microscope images for glycine (**a**,**d**,**g**,**j**), glutamic acid decarboxylase (GAD; **b**,**e**,**h**,**k**) and when both images are merged (**c**,**f**,**i**,**l**). Both lower-magnification images (**a**–**f**) and higher-power images (**g**–**l**) from sections from P5 (**a**–**c**, **g**–**i**) and P18 rats (**d**–**f**, **j**–**l**) are shown. At P5, there is weak glycine immunoreactivity throughout the LSO but intense GAD immunoreactivity (**a**–**c**). The high-power images (**g**–**i**) further show that only a few glycine-positive puncta exist in the LSO, whereas there are numerous GAD-positive puncta. At P18, the low-power images (**d**–**f**) show the intense glycine immunoreactivity and the weak GAD immunoreactivity in the LSO. The high-power images (**j**–**l**) reveal that many glycine-positive puncta are present in the LSO, but there are only a few GAD-positive puncta. Arrowheads indicate example boutons containing both glycine and GAD immunoreactivity. The scale bar in **a** applies to the low-power images (**a**–**f**; 100 μm); the scale bar in **g** applies to the high-power images (**g**–**l**; 10 μm). Under our experimental conditions, soma staining for GAD and glycine in the LSO neurons is not shown as clearly as that for the presynaptic boutons. Staining and image-capturing conditions were optimized for visualization of boutons.

decay time course of the mixed mIPSCs. Our preliminary data indicate that VIAAT is expressed at relatively high levels in the rat LSO. A change in the content of neurotransmitter, from noradrenaline to acetylcholine, has also been found in peripheral sympathetic nerve terminals following innervation of their targets in the sweat gland[22,23]. A switch from GABA to glycine has already been reported for IPSCs evoked by stimulation of multiple MNTB inputs[8–11], but here we provide new evidence that neurotransmitter switching at a central synapse can occur at the level of a single presynaptic vesicle.

One intriguing result from the present study is that although the switch from GABAergic to glycinergic eIPSCs was evident at P7 (**Fig. 1**) and there was a decline in the proportion of GABAergic mIPSCs over the same period, the contribution of GABA to the mixed mIPSCs did not significantly decrease until after the second postnatal week (**Fig. 4**). One possible explanation for this difference is that switching of terminal and vesicle neurotransmitter content may occur over a shorter time period in individual terminals, but these effects in a population of terminals may not be apparent until later. For example, pure GABAergic terminals may be converted to a mixed phenotype in the first postnatal week, while at the same time, other mixed terminals are converted to pure glycinergic terminals (and hence would no longer be included in the population of mixed mIPSCs). If such temporal heterogeneity does occur, one may not expect to see changes in the population responses until all the terminals had already showed significant switching.

Presynaptic changes in neurotransmitter content, that is, an increase in glycine and a decrease in GABA, can be added to the range of changes in inhibitory synaptic transmission and its modulation that have been reported in the LSO throughout development. Morphological changes include extensive remodeling of pre- and postsynaptic elements. In the first postnatal week, expansion of MNTB afferents is apparent in the gerbil LSO, and this is followed by a more prolonged period (for up to 4 weeks) of refinement and elimination of both the terminal boutons and the LSO dendrites[10,19]. For the rat LSO, the number of dendritic end-points begins to decline during the first postnatal week, although the most marked decreases in the relative size of LSO dendrites and their fields occurs after P14 (ref. 24). Synapse elimination and functional reorganization of MNTB–LSO connections have also been recently demonstrated in the rat[20]. In this previous study, the functional refinement of the inhibitory inputs was completed by P8, suggesting that functional refinement of the inhibitory inputs may precede structural refinements. The shift from GABAergic to glycinergic eIPSCs in the gerbil occurs slightly later than observed for rat LSO (**Fig. 1**) and MSO inputs[9]—it is only about 40% complete by P8 (ref. 8). If synapse elimination is in fact completed by P8 in the rat, this would further support our hypothesis of changes in transmitter content in preexisting synapses. Our demonstration of mixed mIPSCs also indicates that glycine and $GABA_A$ receptors are colocalized at LSO synapses. Changes in receptors and their associated accessory proteins have also been reported in the developing LSO. Gephyrin immunoreactivity is very low at birth in the gerbil LSO but increases markedly over the first few weeks[8]. Antibody staining for $GABA_A$ receptor subunits β2

and β3 shows a parallel decline over this period[8]. Expression of the glycine α1 receptor subunit increases markedly over the first 2 weeks[10], replacing the neonatal (presumed α2) receptor isoform. This subunit switch is likely to contribute to the briefer decay times of glycinergic mIPSCs over the course of development[25]. The increased amplitude of glycinergic mIPSCs could also reflect changes in subsynaptic receptors, although we did not observe any developmental change in the amplitude of responses to exogenous glycine.

What could be the functional significance of the switch from GABAergic to glycinergic transmission? Both GABA and glycine depolarize neonatal LSO neurons due to their high intracellular Cl^- content[26,27]. The depolarizing GABA/glycine responses in the rat LSO convert to hyperpolarizing responses during the first two postnatal weeks[26]. This occurs because, in more mature neurons, the outwardly directed Cl^- transporter, KCC-2, is integrated into the plasma membrane and becomes functional[28]. The longer-duration GABAergic responses observed in this study and others[9] would be expected to produce a more prolonged depolarization than glycine would produce, thereby allowing greater Ca^{2+} influx. In fact, Ca^{2+} transients in response to MNTB stimulation have been observed in rat and mice LSO neurons during the first postnatal week[29]. The Ca^{2+} transients generated by exogenous GABA were also larger than those generated by exogenous glycine (although the synaptic Ca^{2+} transients were similar for GABAergic and glycinergic inputs)[29]. GABA-induced membrane depolarization in immature neurons has been shown to be important for neuronal maturation[30–32]. The aggregation of glycine receptors by gephyrin, for example, is promoted by Ca^{2+} influx through channels in the postsynaptic membrane[33]. Thus, GABA-induced elevation of Ca^{2+} might be similarly important for insertion of glycine receptors into the subsynaptic membrane in developing LSO neurons.

Another possible contribution from the GABAergic inhibition in the younger rats concerns $GABA_B$ receptor–mediated responses. In LSO neurons from P4–P8 rats, postsynaptic $GABA_B$ receptors mediate a form of frequency-dependent synaptic plasticity[34,35]. Hence GABAergic neurotransmission may also be important in developing LSO neurons due to actions via $GABA_B$ receptors.

In the adult, the briefer hyperpolarizing responses mediated by glycine receptors would be more appropriate for accurate processing of temporal differences in the sound input from both ears. Our results show that, in addition to synaptic remodeling and changes in postsynaptic receptors, changes in the neurotransmitter content of presynaptic terminals and their vesicles also contribute to the developmental switch from GABAergic to glycinergic inhibition in the rat LSO.

METHODS

All experiments were performed in accordance with the Guiding Principles for the Care and Use of Animals approved by the Council of the Physiological Society of Japan.

Electrophysiology. Wistar rats, at 1–17 d after birth (P1–P17), were quickly decapitated under ether anesthesia. Coronal midbrain slices containing the LSO were made (280-350 μm thickness) as previously described[36]. The ionic composition of the internal (patch pipette) solution for the whole-cell recordings contained 50 mM CsCl, 30 mM Cs_2SO_4, 0.5 mM $CaCl_2$, 2 mM $MgCl_2$, 5 mM EGTA, 5 mM TEA-Cl, 5 mM Mg-ATP and 10 mM HEPES. pH was adjusted to 7.2 with Tris-base. QX-314 (5 mM, Research Biochemicals) was added to the internal solution to block voltage-dependent Na^+ channels. The external solution for the brain slice recordings contained 124 mM NaCl, 5 mM KCl, 1.2 mM KH_2PO_4, 1.3 mM $MgSO_4$, 2.4 mM $CaCl_2$, 10 mM glucose, 24 mM $NaHCO_3$, and was well-oxygenated with 95% O_2/5% CO_2.

Single LSO neurons were mechanically dissociated from brain slices, so as to preserve functional presynaptic nerve terminals[15] (**Fig. 2a**). The internal patch-pipette solution for these recordings was as described above. The standard external solution contained 150 mM NaCl, 5 mM KCl, 1 mM $MgCl_2$, 2 mM $CaCl_2$, 10 mM HEPES and 10 mM glucose (pH 7.2). Antagonists and agonists were applied to acutely dissociated LSO neurons using a Y-tube perfusion device[37]. Neurons were pre-incubated with receptor antagonists for at least 30 s before recording data or applying agonists.

Spontaneous mIPSCs were acquired using pClamp 8.2 (Axon Instruments) and analyzed using both pClamp 8.2 and the MiniAnalysis program (Synaptosoft). Events were detected using an amplitude threshold of 2 pA and events were further rejected or accepted on the basis of their rise and decay times. Large numbers of mIPSCs (>200) were obtained from each neuron recording. mIPSC decay time constants were obtained by fitting a double exponential function to the mIPSC decay from the time period corresponding to between 90% and 10% of the peak mIPSC amplitude. Individual events were fitted (with >150 iterations) to the function: $y = y_0 + y_{fast}\, e^{(-x/\tau fast)} + y_{slow}\, e^{(-x/\tau slow)}$. mIPSCs where considered to have a mono-exponential decay when the relative contribution of one of the exponential distributions was <1%. Thus, the decision about whether a single mIPSC decayed with a single or dual components was completely objective. The proportion of GABAergic, glycinergic or mixed mIPSCs, in each recording, was automatically determined from the distribution of mIPSC decays. Numerical values are presented as means ± standard error of the mean (s.e.m.).

Post-embedding immunohistochemistry. Rats were deeply anesthetized with sodium pentobarbital (100 mg per kg body weight) and transcardially perfused with saline, followed by 15 min perfusion with fixative (a mixture of 2.5% glutaraldehyde and 4% paraformaldehyde in 0.1 M phosphate buffer). The brainstem was removed and incubated overnight (4 °C) in the same fixative. Subsequently, small blocks of brainstem, containing the LSO, were treated with 1% OsO_4, dehydrated in ethanol and propylene oxide, and embedded in Durcupan (ACM Fluka). Ultrathin slices were cut and mounted on nickel grids. Postembedding double immunogold labeling of GABA and glycine was performed as described[38]. The GABA antibody (1:8,000, gift of O.P. Ottersen, University of Oslo, Oslo, Norway) was visualized using an IgG coupled to 20 nm gold particles (GAR 20; 1:20, British Biocell International). The glycine antibody (1:1,000, Biogenesis) was visualized using a Fab fragment coupled to 10 nm gold particles (GFAR 10; 1:20, British Biocell International). The ultrathin specimens were initially incubated for GABA immunogold labeling, followed by that for glycine labeling. Specimens were exposed to formaldehyde vapor for 1 h at 80 °C to avoid any interference between the sequential incubations. Specimens only stained positive for the 20 nm gold-conjugated particles when they were incubated with the GABA-specific antibody while the smaller gold-conjugated particles were only observed when specimens contained the glycine-specific antibody (**Supplementary Fig. 2** online). The specificity of the antibodies under our conditions was tested[39]. Brain sections were processed alongside control sections containing a series of different amino acids gluteraldehyde-conjugated to brain macromolecules. For quantification of the amount of presynaptic glycine and GABA we manually counted the number of gold particles observed within presynaptic terminals that could be clearly seen to synapse onto the soma. Many terminals examined contained a low level of staining for GABA and glycine reactive gold particles (1–4 particles/μm^2). A second population contained a greater density of gold particles (**Supplementary Fig. 1** online). The presence of >5 particles/μm^2 was the only criteria used to accept inhibitory terminals for study. To compare particle density across different terminals and specimens, results are expressed as particles/μm^2. Three rats from each age group were used and the specimens derived from rats at the two different ages were grouped together. Sections contained terminals that synapsed on to the soma, or on the larger proximal dendrites.

Immunocytochemistry. Rats were deeply anesthetized with sodium pentobarbital (100 mg/kg body weight), and then were transcardially perfused with phosphate buffered saline (PBS, pH 7.4) followed by a mixture of 2% paraformaldehyde and 2.5% glutaraldehyde in 0.1 M phosphate buffer (pH 7.4). The brains were left *in situ* for 1–2 h at room temperature (22–24 °C) and then were removed from the skull. Small blocks containing the LSO were separated from the brain and then sliced transversely into 50 μm-thick serial sections. The thin sections were incubated in 30% sucrose in 0.1 M phosphate buffer (pH 7.4) for 1 h, and were then freeze-thawed in liquid nitrogen.

No detergents were used, as they can reduce the degree of glutamic acid decarboxylase (GAD) immunostaining. Slices were then incubated overnight in PBS containing 1% bovine serum albumin and 0.05% sodium azide, before being incubated in mixture of rabbit polyclonal anti-glycine antibody (1:10,000; Chemicon) and goat polyclonal S3 antibody against GAD (1:2,000; NIMH Laboratory of Clinical Science) for 5 d at 20 °C. The S3 antibody recognizes both GAD65 and GAD67 forms[40]. After this, the sections were rinsed briefly in PBS, and then incubated with a mixture of fluorescein isothiocyanate (FITC)-conjugated donkey anti-rabbit antibody (1:1,000; Jackson Immunoresearch) and rhodamine red-conjugated donkey anti-goat antibody (1:1,000; Jackson Immunoresearch) for 3 h. The sections were rinsed briefly in PB, mounted in Vectashield (Vector Laboratories) and examined with a confocal laser-scanning microscope (CLSM; TCS-SP2; Leica). Single laser beams, of 488 and 543 nm in wavelength, were alternately focused on to the specimen to collect fluorescent images for FITC (glycine) and rhodamine red (GAD), respectively. In the absence of the primary antibodies, only negligible background staining was observed in the LSO (data not shown), confirming the specificity of our GAD and glycine immunolabeling.

Note: Supplementary information is available on the Nature Neuroscience website.

ACKNOWLEDGMENTS

We thank A. Moorhouse for discussion and editing of the manuscript, and N. Akaike for technical advice. We also thank O.P. Otterson, I.J. Kopin, W.H. Oertel, D.E. Schmechel and M.L. Tappaz for help obtaining antibodies. This work was supported by research grants from the Ministry of Education, Culture, Sports, Science and Technology, Japan (15016082, 15650076 and 15390065 to J.N).

COMPETING INTERESTS STATEMENT

The authors declare that they have no competing financial interests.

Received 4 July; accepted 1 December 2003
Published online at http://www.nature.com/natureneuroscience/

1. Ornung, G. *et al*. Qualitative and quantitative analysis of glycine- and GABA-immunoreactive nerve terminals on motoneuron cell bodies in the cat spinal cord: a postembedding electron microscopic study. *J. Comp. Neurol.* **365**, 413–426 (1996).
2. Yang, H.W., Min, M.Y., Appenteng, K. & Batten, T.F. Glycine-immunoreactive terminals in the rat trigeminal motor nucleus: light- and electron-microscopic analysis of their relationships with motoneurones and with GABA-immunoreactive terminals. *Brain Res.* **749**, 301–319 (1997).
3. Levi, S., Chesnoy-Marchais, D., Sieghart, W. & Triller, A. Synaptic control of glycine and $GABA_A$ receptors and gephyrin expression in cultured motoneurons. *J. Neurosci.* **19**, 7434–7449 (1999).
4. Kneussel, M. & Betz, H. Receptors, gephyrin and gephyrin-associated proteins: novel insights into the assembly of inhibitory postsynaptic membrane specializations. *J. Physiol.* **525**, 1–9 (2000).
5. O'Brien, J.A. & Berger, A.J. Cotransmission of GABA and glycine to brain stem motoneurons. *J. Neurophysiol.* **82**, 1638–1641 (1999).
6. Jonas, P., Bischofberger, J. & Sandkuhler, J. Co-release of two fast neurotransmitters at a central synapse. *Science* **281**, 419–424 (1998).
7. Russier, M., Kopysova, I.L., Ankri, N., Ferrand, N. & Debanne, D. GABA and glycine co-release optimizes functional inhibition in rat brainstem motoneurons *in vitro*. *J. Physiol.* **541**,123–137 (2002).
8. Kotak, V.C., Korada, S., Schwartz, I.R. & Sanes, D.H. A developmental shift from GABAergic to glycinergic transmission in the central auditory system. *J. Neurosci.* **18**, 4646–4655 (1998).
9. Smith, A.J., Owens, S. & Forsythe, I.D. Characterization of inhibitory and excitatory postsynaptic currents of the rat medial superior olive. *J. Physiol.* **529**, 681–698 (2000).
10. Sanes, D.H. & Friauf, E. Development and influence of inhibition in the lateral superior olivary nucleus. *Hear. Res.* **147**, 46–58 (2000).
11. Korada, S. & Schwartz, I.R. Development of GABA, glycine, and their receptors in the auditory brainstem of gerbil: a light and electron microscopic study. *J. Comp. Neurol.* **409**, 664–681 (1999).
12. del Castillo, J. & Katz, B. Quantal components of end-plate potential. *J. Physiol.* **124**, 560–573 (1954).
13. Walmsley, B., Alvarez, F.J. & Fyffe, R.E. Diversity of structure and function at mammalian central synapses. *Trends Neurosci.* **21**, 81–88 (1998).
14. Akaike, N. & Moorhouse, A.J. Techniques: applications of the nerve-bouton preparation in neuropharmacology. *Trends Pharmacol. Sci.* **24**, 44–47 (2003).
15. Dumoulin, A., Triller, A. & Dieudonne, S. IPSC kinetics at identified GABAergic and mixed GABAergic and glycinergic synapses onto cerebellar Golgi cells. *J. Neurosci.* **21**, 6045–6057 (2001).
16. Keller, A.F., Coull, J.A., Chery, N., Poisbeau, P. & De Koninck, Y. Region-specific developmental specialization of GABA-glycine cosynapses in laminas I-II of the rat spinal dorsal horn. *J. Neurosci.* **21**, 7871–7880 (2001).
17. Friauf, E, Hammerschmidt, B. & Kirsch, J. Development of adult-type inhibitory glycine receptors in the central auditory system of rats. *J. Comp. Neurol.* **385**, 117–134 (1997).
18. Otis, T.S., De Koninck, Y. & Mody, I. Lasting potentiation of inhibition is associated with an increased number of gamma-aminobutyric acid type A receptors activated during miniature inhibitory postsynaptic currents. *Proc. Natl. Acad. Sci. USA* **91**, 7698–7702 (1994).
19. Sanes, D.H. & Siverls, V. Development and specificity of inhibitory terminal arborizations in the central nervous system. *J. Neurobiol.* **22**, 837–854 (1991).
20. Kim, G. & Kandler, K. Elimination and strengthening of glycinergic/GABAergic connections during tonotopic map formation. *Nat. Neurosci.* **6**, 282–290 (2003).
21. Gasnier, B. The loading of neurotransmitters into synaptic vesicles. *Biochimie* **82**, 327–337 (2000).
22. Schotzinger, R.J. & Landis, S.C. Cholinergic phenotype developed by noradrenergic sympathetic neurons after innervation of a novel cholinergic target *in vivo*. *Nature* **335**, 637–639 (1988).
23. Habecker, B.A., Tresser, S.J., Rao, M.S. & Landis, S.C. Production of sweat gland cholinergic differentiation factor depends on innervation. *Dev. Biol.* **167**, 307–316 (1995).
24. Rietzel, H.J. & Friauf, E. Neuron types in the rat lateral superior olive and developmental changes in the complexity of their dendritic arbors. *J. Comp. Neurol.* **390**, 20–40 (1998).
25. Takahashi, T., Momiyama, A., Hirai, K., Hishinuma, F. & Akagi, H. Functional correlation of fetal and adult forms of glycine receptors with developmental changes in inhibitory synaptic receptor channels. *Neuron* **9**, 1155–1161 (1992).
26. Kakazu, Y., Akaike, N., Komiyama, S. & Nabekura, J. Regulation of intracellular chloride by cotransporters in developing lateral superior olive neurons. *J. Neurosci.* **19**, 2843–2851 (1999).
27. Kandler, K. & Friauf E. Development of glycinergic and glutamatergic synaptic transmission in the auditory brainstem of perinatal rats. *J. Neurosci.* **15**, 6890–6904 (1995).
28. Balakrishnan, V. *et al*. Expression and function of chloride transporters during development of inhibitory neurotransmission in the auditory brainstem. *J. Neurosci.* **23**, 4134–4145 (2003).
29. Kullmann, P.H., Ene, F.A. & Kandler, K. Glycinergic and GABAergic calcium responses in the developing lateral superior olive. *Eur. J. Neurosci.* **15**, 1093–1104 (2002).
30. Gao, B.X. & van den Pol, A.N. GABA, not glutamate, a primary transmitter driving action potentials in developing hypothalamic neurons. *J. Neurophysiol.* **85**, 425–434 (2001).
31. Ganguly, K., Schinder, A.F., Wong, S.T. & Poo, M. GABA itself promotes the developmental switch of neuronal GABAergic responses from excitation to inhibition. *Cell* **105**, 521–532 (2001).
32. Lauder, J.M., Liu, J., Devaud, L. & Morrow, A.L. GABA as a trophic factor for developing monoamine neurons. *Perspect. Dev. Neurobiol.* **5**, 247–259 (1998).
33. Kirsch, J. & Betz, H. Glycine-receptor activation is required for receptor clustering in spinal neurons. *Nature* **392**, 717–720 (1998).
34. Kotak, V.C., DiMattina, C. & Sanes, D.H. $GABA_B$ and Trk receptor signaling mediates long-lasting inhibitory synaptic depression. *J. Neurophysiol.* **86**, 536–540 (2001).
35. Chang, E.H., Kotak, V.C. & Sanes, D.H. Long-term depression of synaptic inhibition is expressed postsynaptically in the developing auditory system. *J. Neurophysiol.* **90**, 1479–1788 (2003).
36. Kakazu, H., Uchida, S., Nakagawa, T., Akaike, N. & Nabekura, J. Reversibility and cation selectivity of K^+-Cl^- cotransport in rat CNS Neurons. *J. Neurophysiol.* **84**, 281–288 (2000).
37. Nabekura J., Omura T. & Akaike N. Alpha2 adrenoceptor potentiates glycine receptor-mediated taurine response through protein kinase A in rat substantia nigra neurons. *J. Neurophysiol.* **76**, 2447–2454 (1996).
38. Matsubara, A., Laake, J.H., Davanger, S., Usami, S. & Ottersen, O. P. Organization of AMPA receptor subunits at a glutamate synapse: a quantitative immunogold analysis of hair cell synapses in the rat organ of Corti. *J. Neurosci.* **16**, 4457–4467 (1996).
39. Ottersen, O.P., Zhang, N. & Walberg, F. Metabolic compartmentation of glutamate and glutamine morphological evidence obtained by quantitative immunocytochemistry in rat cerebellum. *Neuroscience* **46**, 519–534 (1992).
40. Kaufman, D.L., McGinnis, J.F., Krieger, N.R. & Tobin, A.J. Brain glutamate decarboxylase cloned in lambda gt-11: fusion protein produces gamma-aminobutyric acid. *Science* **232**, 1138–1140 (1986).